Spontaneous emergence of milling (vortex state) in a Vicsek-like model

Costanzo, A; Hemelrijk, C K

Published in:
Journal of Physics D: Applied Physics

DOI:
10.1088/1361-6463/aab0d4

Publication date:
2018

Spontaneous emergence of milling (vortex state) in a Vicsek-like model

A Costanzo & C K Hemelrijk

Rijksuniversiteit Groningen, Faculty of Science and Engineering
Groningen Institute for Evolutionary Life Sciences (GELIFES)
Nijenborgh 7, 9747 AG Groningen, The Netherlands

E-mail: andreacostanzo881@gmail.com

October 2017

Abstract. Collective motion is of interest to laymen and scientists in different fields. In groups of animals, many patterns of collective motion arise such as polarized schools and mills (i.e. circular motion). Collective motion can be generated in computational models of different degrees of complexity. In these models moving individuals coordinate with others nearby. In the more complex models, individuals are attracting each other, aligning their headings, and avoiding collisions. Simpler models may include only one or two of these types of interactions. The collective pattern that interests us here is milling, which is observed in many animal species. It has been reproduced in the more complex models, but not in simpler models that are based only on alignment, such as the well-known Vicsek model. Our aim is to provide insight in the minimal conditions required for milling by making minimal modifications to the Vicsek model. Our results show that milling occurs when both the field of view and the maximal angular velocity are limited. Remarkably, apart from milling, our minimal model also exhibits many of the other patterns of collective motion observed in animal groups.

PACS numbers: 87.10.-e, 87.10.Mn, 05.65.+b, 45.50.-j, 64.60.-i

Keywords: Collective behaviour, Vicsek model, Milling, Self-propelled particles

1. Introduction

Collective phenomena of self-propelled particles have recently attracted wide and interdisciplinary scientific interest [1]. In nature many different eye-catching patterns of collective motion are observed in groups of animals such as flocks of birds and schools of fish: for instance, animals form polarized groups of different shapes, like travelling bands and mills (i.e. circular motion) [1, 2, 3, 4].

Collective motion has been represented in computational models of different degrees of complexity. In these models, moving individuals coordinate with others nearby. More complex models are based on mutual attraction, alignment of headings, and avoidance of collisions with others [1, 5, 6, 7]. Simpler models comprise only one or two of these types of interactions [8, 9, 10, 11, 12, 13, 14]. We focus on a particular pattern of collective motion, milling, that arises in fish schools and also in other species, like for example ants. It is a rotating circular formation of animals, where individuals turn around a common center, also referred to as circular motion and vortex state [15, 16]. Its function is still unclear [17].

Milling has been observed to emerge in models of collective motion based on avoidance, alignment, and attraction (so-called zonal models, because concentric rings around particles define zones of avoidance, alignment and attraction) [5, 17, 18, 19], in models using distance-dependent interaction-potentials that give rise to attractive and repulsive forces [20, 21, 22, 23, 24, 25], in models with attraction and speed-dependent alignment [8], and in models including only attraction [9, 10, 11].

In all these cases the space in which individuals move is free of confining walls. In such environments, milling has not (yet) been shown in models which include only alignment interactions. In these models, collective circular motion has been shown only if particles are confined by circular walls, and circular motion emerges due to the alignment interaction with the walls [26, 27]. There are several models of self-propelled particle dynamics with only alignment [26, 28, 29]. The well-known Vicsek model is famous for its phase transition from the disordered phase (in which all particles head in random directions) to the ordered phase (in which all particles move collectively in a single direction) [28].

The objective of the present study is to investigate whether milling emerges after modifying the original Vicsek model (without walls) [28]. We show that by introducing a limited field of view and a bounded maximal angular velocity of particles, particles form stable mills. Our modified model also generates a variety of patterns of collective motion beyond milling, such as bands, lines, and fronts.

2. Model

Our model is a two-dimensional model with periodic boundary conditions; it is a modified version of the Vicsek model, which we here briefly recall.

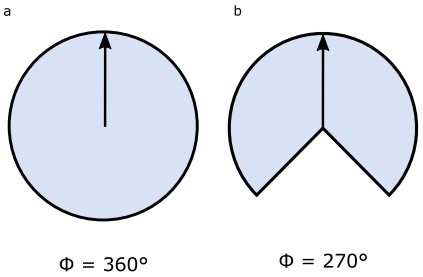

Figure 1. Sketch of the field of view ϕ. a) Vicsek model: particles have an all-round field of view. b) Modified Vicsek model: particles have a blind angle behind them. Black arrows represent the orientation θ of particles.

2.1. The Vicsek model

N point-particles move continuously (off-lattice) on a two dimensional square of lateral size L with periodic boundary conditions. The particles are characterized by their position $\mathbf{x}_i$ and their orientation given by the angle $\theta_i \in [0°, 360°)$. The starting configuration is with particles at random positions with random orientations. Particles move at constant speed v in direction of their orientation θ_i. Particles interact with other particles if they are closer than the interaction range r, which we choose as unit of length ($r = 1$). The time unit is the time interval between two updates of positions and orientations, $\Delta t = 1$. The equation of motion reads:

$$\mathbf{x}_i(t + \Delta t) = \mathbf{x}_i(t) + \mathbf{v}_i(t)\Delta t \tag{1}$$

where $\mathbf{v}_i$ is the velocity vector with speed v and orientation θ_i. The orientation updates as follows:

$$\theta_i(t + \Delta t) = \langle\theta_j(t)\rangle_r + \Delta\theta_i \tag{2}$$

where $\langle\theta_j(t)\rangle_r$ denotes the average orientation of particles (including particle i) at distance smaller than r (interaction range) from particle i, and where $\Delta\theta_i$ represents the rotational noise, which is a random variable uniformly distributed in the interval $[-\eta/2, \eta/2]$. The motion of particles is updated synchronously, i.e. first all average orientations are computed and then particles are moved. The free parameters of the Vicsek model are the speed v, the noise η, and the density $\rho = N/L^2$.

2.2. The modified Vicsek model

In order to obtain milling, we modify two parameters:

(i) Field of view $\phi \in [0°, 360°]$:
In the Vicsek model particles interact with all other particles that are around them (Figure 1a). We limit the field of view ϕ, such that particles will have a blind angle behind them (Figure 1b).

(ii) Maximal angular velocity $\omega \in [0°/\Delta t, 180°/\Delta t]$:
In the Vicsek model there is no limitation on the angle particles can turn by (i.e.

$\omega = 180°/\Delta t$). Here, we limit the particle rotation to the maximal angular velocity ω.

Thus, equation 2 becomes

$$\theta_i(t+\Delta t) = \begin{cases} \langle\theta_j(t)\rangle_{r,\phi} + \Delta\theta_i & \text{for } |\Delta\Theta_i| < \omega\Delta t \\ \theta_i(t) + \omega\Delta t + \Delta\theta_i & \text{for } \Delta\Theta_i \geq \omega\Delta t \\ \theta_i(t) - \omega\Delta t + \Delta\theta_i & \text{for } \Delta\Theta_i \leq -\omega\Delta t \end{cases} \quad (3)$$

where $\langle\theta_j(t)\rangle_{r,\phi}$ denotes the average orientation of particles in the interaction range $r = 1$ *and* in the field of view ϕ (including particle i), and where $\Delta\Theta_i \in [-180°, 180°]$ is the difference in orientation between the current orientation and the average orientation of the interacting particles (note that, if for example the current orientation $\theta_i = 10°$ and the average orientation of the interacting particles $\langle\theta_j(t)\rangle_{r,\phi} = 350°$, then $\Delta\Theta_i = -20°$).

At $v = 0$ particles are not moving. For $v \to \infty$ we get complete mixing, and thus no milling. Therefore, in order to obtain milling, the speed has to be low enough ($v\Delta t/r \ll 1$) (see Figure A1 in the Appendix). Thus, the free parameters of the modified Vicsek model are the ratio of speed over maximal angular velocity $v/(r\omega)$ (made adimensional dividing by $r = 1$), the field of view ϕ, the density ρ, and the noise η.

We simulate the motion of N particles (up to $N = 2000$ at density $\rho = N/L^2 = 5$) in a quadratic box of size $L = 20$ (value chosen after having studied finite size effects, see Section 3.1 and Figure 2). In the following, speed is expressed in units of $r/\Delta t$, and angular velocity is expressed in degrees per time unit ($°/\Delta t$). If not stated differently, we vary the ratio between speed and maximal angular velocity $v/(r\omega)$ keeping $\omega = 10$ and varying the speed in the interval $[0.05, 0.35]$. In this way, for a given noise, we keep the ratio between noise and maximal angular velocity $\eta\Delta t/\omega$ (made adimensional by multiplying by Δt) constant.

2.3. Measured quantities

We quantify milling by two quantities: the absolute value of the average normalized velocity (the polar order parameter)

$$v_a = \frac{1}{N}|\sum_{i=1}^{N} \mathbf{u}_i| \quad (4)$$

($\mathbf{u}_i = \mathbf{v}_i/v$ is the velocity unit vector), which is equal to one when all the particles move in the same direction and zero when particles move in random directions, and the average absolute value of the normalized angular momentum

$$m_a = \frac{1}{N}\sum_{i=1}^{N} \frac{|\mathbf{r}_{cm,i} \times \mathbf{u}_i|}{|\mathbf{r}_{cm,i}|} \quad (5)$$

(note that in our model there are no masses and thus no mass is present in our definition of angular momentum, and that since we consider two dimensions, the absolute value of the cross product reads $|\mathbf{a} \times \mathbf{b}| = |a_1 b_2 - a_2 b_1|$) where $|\mathbf{r}_{cm,i}| = |\mathbf{r}_i - \mathbf{r}_{cm}|$ is the distance

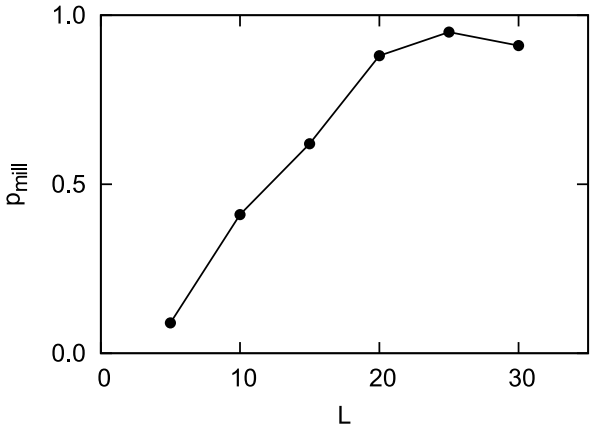

Figure 2. Milling proportion p_{mill} as a function of system size L, (computed over 100 runs, at $\phi = 180°$, $v/(\omega r) = 0.86$, $\eta\Delta t/\omega = 0.5$, $\rho = 2.5$).

of particle i to the center of mass of its cluster (or animal group). A cluster is defined as a set of particles where the distance between particles is smaller than $d_c = 0.5$. Thus, d_c is the pairwise distance used to judge whether two particles belong to the same cluster.

The value of d_c has been chosen such that particles belonging to the same mill are assigned to a single cluster, and particles belonging to different mills are assigned to different clusters (i.e. in order to obtain a one-to-one correspondence between clusters and mills). For this, we need to know the radius of mills. Our simulations show these radii to be always close to the interaction range $r = 1$. A very small value of d_c (like $d_c = 0.1$) results in particles which belong to the same mill not being assigned to the same cluster. In the rare case of two mills being located very close together, for instance with their centers at distance 3 (such that the distance between particles of different mills can reach the value of 1, since the radius of the mill is 1), $d_c = 1$ would classify particles of the two different mills to a single cluster. Using a smaller value of d_c prevents this error. Therefore we arbitrarily choose $d_c = 0.5$.

m_a ranges from zero to one, and will be close to one when particles rotate in mills. In order to detect particles rotating in mills, a threshold on m_a alone does not suffice: for instance, when particles form bands (Figure 8d), $m_a \simeq 0.9$ and $v_a \simeq 1.0$. A configuration with random positions and random orientation gives $m_a \simeq 0.6$ and $v_a \simeq 0$. When particles rotate in mills the average momentum is high *and* the average velocity is low, $m_a > 0.75$ *and* $v_a < 0.5$ (see Figure A2).

For each parameter setting, if not stated differently, we run 10 simulations for 2000 time steps, and measure the described quantities taking a time average over the last 500 steps (after 1500 steps the stationary state has been reached, see Figure A3). The milling proportion p_{mill} is the number of runs where the system is in the milling state divided by the total number of runs.

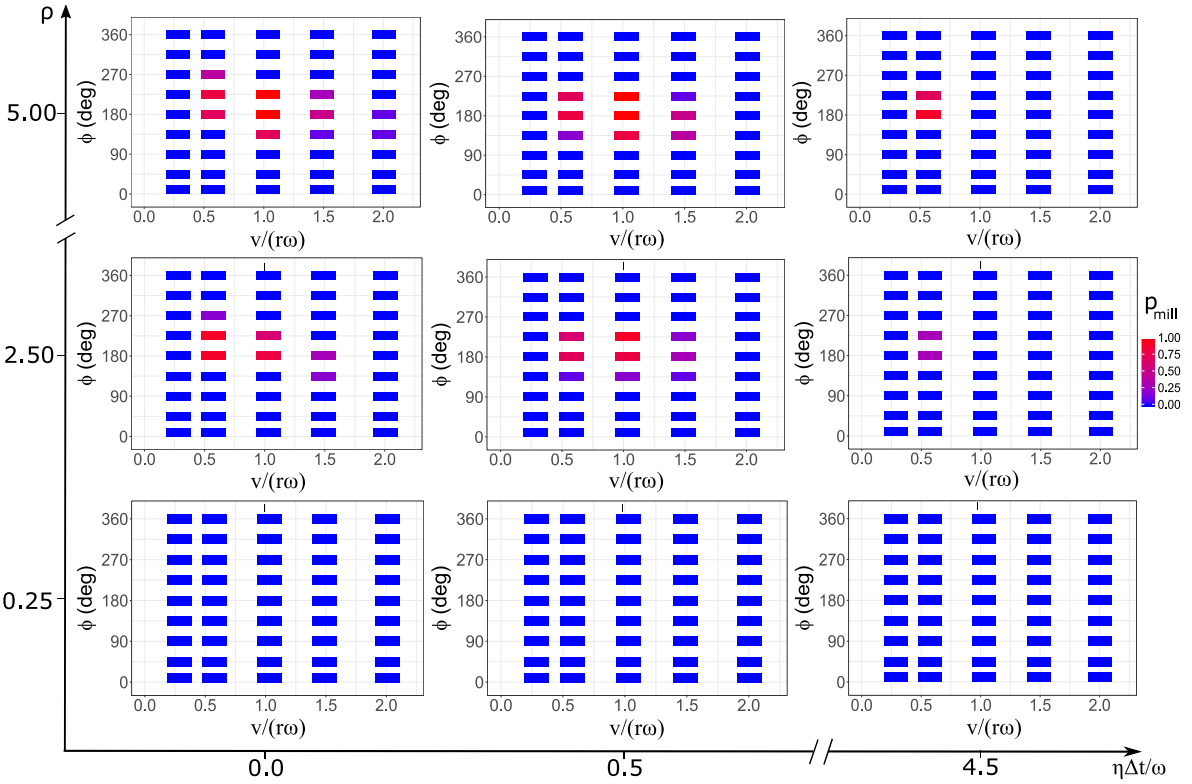

Figure 3. Milling proportion p_{mill} as a function of the field of view ϕ and the ratio between speed and maximal turning angle $v/(r\omega)$ (we vary v and keep $\omega = 10°/\Delta t$ constant), for different noise and density values.

3. Results

3.1. Finite size effects

The modified Vicsek model with a limited field of view $\phi = 180°$ and a maximal angular velocity of $\omega = 10°/\Delta t$, shows spontaneous emergence of milling. In order to choose the system size for a detailed analysis the model exploring the parameter space, we perform a preliminary study on finite size effects on milling. We measure the proportion of milling p_{mill} as a function of system size L (at field of view $\phi = 180°$, speed to maximal angular velocity ratio $v/(\omega r) = 0.86$, noise to maximal angular velocity ratio $\eta\Delta t/\omega = 0.5$, and density $\rho = 2.5$). The proportion of milling increases for $L \leq 20$ and stays constant for $L \geq 20$ (Figure 2), such that $L = 20$ is the smallest system size which can be utilised to study milling.

3.2. Milling

We investigate the modified Vicsek model measuring the milling proportion p_{mill} as a function of the field of view ϕ and the ratio between speed and maximal angular velocity $v/(r\omega)$ (for different noise and density values). The milling proportion is high at intermediate field of view ($\phi \simeq 200°$) and when $v/(r\omega) \simeq 1$ (Figure 3 and Figure 4).

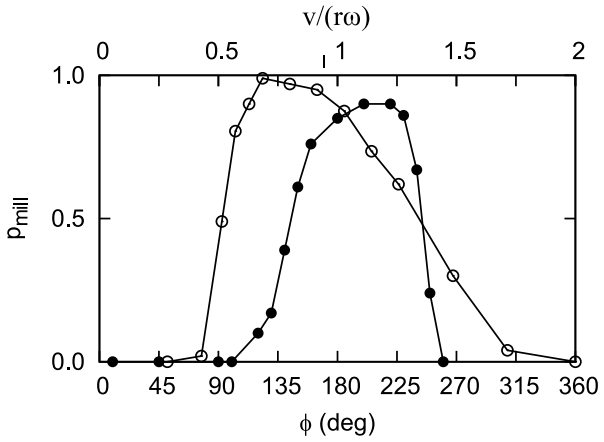

Figure 4. Milling proportion p_{mill} (computed over 200 runs) as a function of the field of view ϕ (at $\eta\Delta t/\omega = 0.5$, $\rho = 2.5$, $v/(r\omega) = 1.03$) (full circles), and milling proportion p_{mill} as a function of the ratio of speed over maximal angular velocity $v/(r\omega)$ (at $\eta\Delta t/\omega = 0.5$, $\rho = 2.5$, $\phi = 180°$) (empty circles).

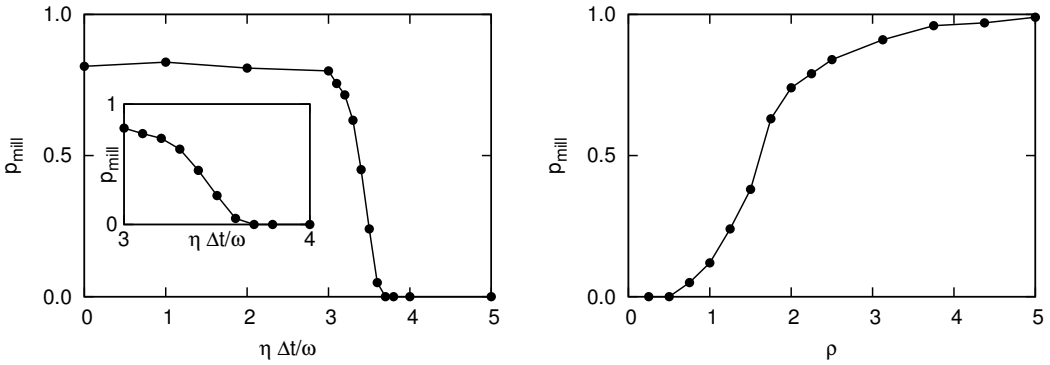

Figure 5. Milling proportion p_{mill} (computed over 200 runs) at $\phi = 180°$, $\omega = 10°$, $v/(\omega r) = 1.03$. Left: as a function of noise (ratio noise over maximal turning angle $\eta\Delta t/\omega$, $\rho = 2.5$) (Inset: zoom on same data). Right: as a function of density ρ ($\eta\Delta t/\omega = 0.5$).

Similar to the original Vicsek model, decreasing noise or increasing density leads to a phase transition. In the original model this was a phase transition from the unordered to the ordered state, in its modified version, it is a phase transition from the state of non-milling to that of milling (Figure 5).

The number of mills that emerge spontaneously varies among different runs (with same parameters). A single mill can emerge or multiple mills can emerge (which may be also counter-rotating). The radius R of the mills is always of the order of magnitude of the interaction range ($R \sim r$, see Figure A3), and does not depend on the size L of the system.

In order to give an intuitive explanation of the parameter range in which milling emerges, we consider the ideal case of four particles placed at positions $x_1 = (R, 0), x_2 = (0, R), x_3 = (-R, 0), x_4 = (0, -R)$, with orientations $\theta_1 = 90°, \theta_2 = 180°, \theta_3 = 270°, \theta_4 =$

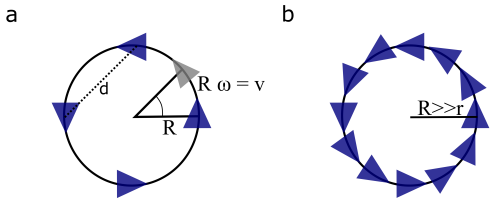

Figure 6. Sketch of the ideal starting configurations for milling: a) For $N = 4$ particles the speed v, the angular velocity ω, and the milling radius R have to satisfy the condition $v/(R\omega) \simeq 1$. The distance between particles is $d = R\sqrt{2}$, and thus the milling radius has to be smaller than $r/\sqrt{2}$. b) For $N \gg 1$, mills with larger radius ($R \gg r$) made by many more particles could exist. Starting from random configurations, we mostly observe mills of radius $R \simeq r$, since it is more likely that particles assume a configuration similar to (a) rather than a configuration similar to (b).

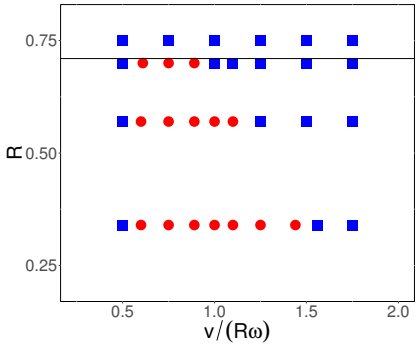

Figure 7. Emergence of milling in the ideal starting configuration of four particles that are moving without noise: milling (circles) and no-milling (squares) as a function of initial radius R and $v/(R\omega)$, ($v = 0.03$, $\phi = 180°$).

0° (Figure 6A). In order to interact with other particles, the radius of the mill R has to be smaller than $r/\sqrt{2}$, where $r = 1$ is the interaction range (our unit of length), since the smallest distance between particles is $R\sqrt{2}$.

At field of view $\phi = 360°$, particles interact with all the others, resulting in an average orientation of zero, and in straight motion of all particles. Thus, a smaller field of view is needed. For field of view $90° < \phi < 270°$, each particle interacts with only two particles, and the desired direction will be 90° to the left. (If the maximal angular velocity ω is smaller than 90°, the particle will rotate to the left by ω.)

In any uniform circular motion, and thus also to obtain milling, the relation

$$R = v/\omega \tag{6}$$

between the radius R, the speed v, and the angular velocity ω must be satisfied. At $v = 0.03$, $\omega = 5$, $R = 0.34$, such that $v/(R\omega) = 1$, without noise, the four particles show milling for field of view $\phi \in [105°, 265°]$ (data not shown). At field of view $\phi = 180°$, without noise, $v = 0.03$, and $R = 0.34$, the four particle case shows milling for $0.5 < v/(R\omega) < 1.5$, while increasing the milling radius to $R = 0.7$ we get milling

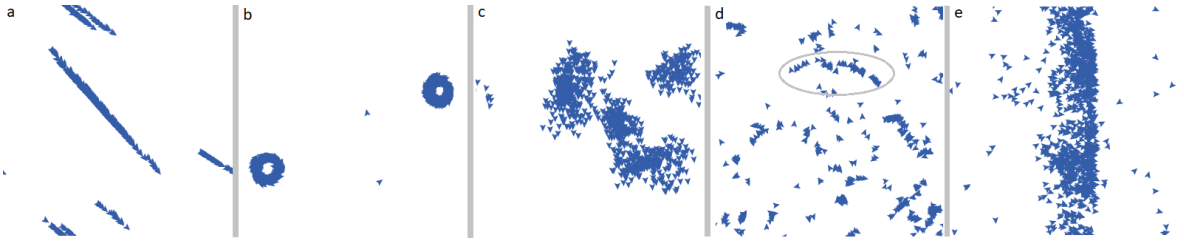

Figure 8. Snapshots of simulations ($N = 1000$, $L = 20$, $\rho = 2.5$): a) Lines ($\phi = 10°$, $v/(r\omega) = 1.03$, $\eta\Delta t/\omega = 0$), b) Mills ($\phi = 180°$, $v/(r\omega) = 1.03$, $\eta\Delta t/\omega = 0.5$), c) Flocks ($\phi = 360°$, $v/(r\omega) = 1.03$, $\eta\Delta t/\omega = 0.5$), d) Fronts ($\phi = 10°$, $v/(r\omega) = 0.29$, $\eta\Delta t/\omega = 0.5$), e) Bands ($\phi = 180°$, $v/(r\omega) = 2.00$, $\eta\Delta t/\omega = 4.5$).

for a smaller range of maximal angular velocity, $0.5 < v/(R\omega) < 1.0$ (Figure 7). The value of $v/(R\omega)$ can also slightly differ from one, since in the four-particle case milling is not always an uniform circular motion, but the milling radius can actually oscillate.

The ideal case with four particles shows that the field of view has to be smaller than that of the Vicsek model ($\phi < 360°$), and that the milling radius R has to be smaller than the interaction range r, $R < r/\sqrt{2} < r$. Furthermore, it shows that the quantity $v/(r\omega)$ has to be close to one.

Yet, we can imagine a mill with larger radius ($R \gg r$) made by many more particles (Figure 6b). Given the circle radius R and the number of particles N, the distance between particles d is given by trigonometric relations, and must be smaller than the interaction range $r = 1$, it reads $d = \sqrt{2R^2(1 - \cos(\gamma))}$, where $\gamma = 360°/N$ is the angle formed by two neighboring particles and the center of the circle. At $R = 70$, with $N = 70$ particles, and at $v/(\omega R) = 1$, milling emerges for $\phi \in [10°, 355°]$.

Starting from a random configuration, it is though more likely that only four particles assume a configuration of milling similar to Figure 6a, rather than that many particles do so (Figure 6b). That is why the observed milling radii are of the same order of magnitude of the interaction range, $R \simeq r$.

3.3. Other emergent patterns of collective motion

Besides milling, in nature, animal groups show many other collective patterns [1]. Most are seen also in our minimal model (Figure 8). These different patterns are stable, and their emergence depends on density, noise, field of view and ratio of speed to angular velocity (Figure 9). For instance, at density $\rho = 2.5$ and without noise ($\eta = 0$), we observe lines (particles moving in the same direction one behind the other, Figure 8a) at small field of view ($\phi \simeq 10°$). These emerge because particles align only with particles in front of them. Mills (Figure 8b) emerge at intermediate field of view and intermediate ratio of speed to maximal angular velocity ($\phi \simeq 180°$, $0.5 \leq v/(r\omega) \leq 1.5$). For other values of field of view and ratio of speed to maximal angular velocity, we observe polarized groups (Figure 8c).

Increasing the ratio of noise to maximal angular velocity to $\eta\Delta t/\omega = 0.5$, causes

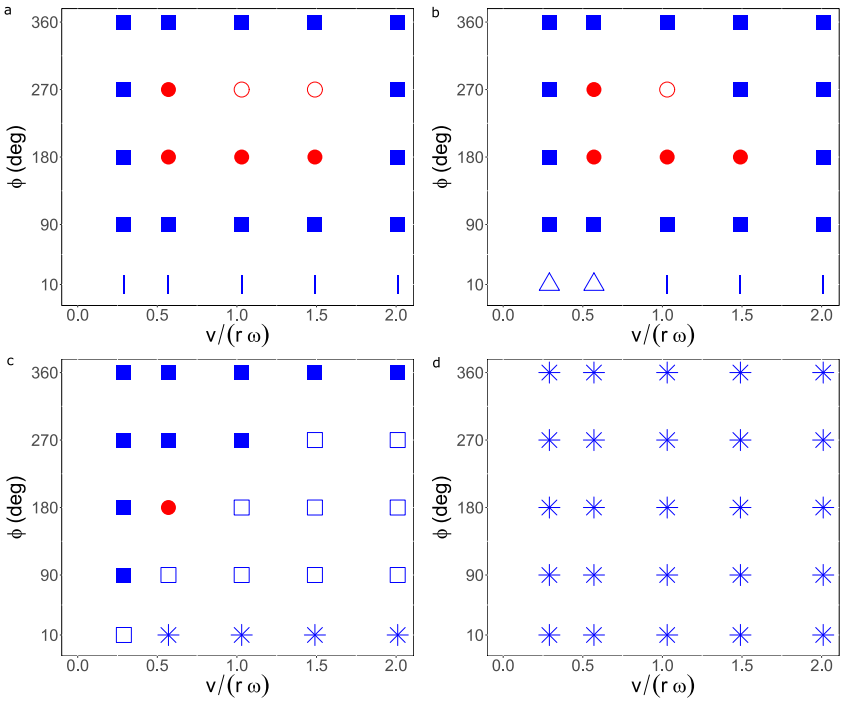

Figure 9. Phase diagrams as a function of the field of view ϕ and the ratio between speed and maximal angular velocity, $v/(r\omega)$. For density $\rho = 2.5$ and different noise values: $\eta\Delta t/\omega = 0$ (a), $\eta\Delta t/\omega = 0.5$ (b), $\eta\Delta t/\omega = 4.5$ (c), $\eta\Delta t/\omega = 9.0$ (d). Vertical lines: lines, full circles: stable milling, empty circles: unstable milling, full squares: flocks, triangles: fronts, empty squares: bands, stars: disordered state.

particles to rotate more, and therefore, at low ratio of speed to maximal angular velocity, fronts emerge (particles originally in small groups, splitting, Figure 8d and 9b). At higher speed lines are still present. Increasing the ratio of noise to maximal angular velocity from $\eta\Delta t/\omega = 0.5$ to $\eta\Delta t/\omega = 4.5$, lines and fronts disappear, while bands (particles moving in the same direction one next to the other, Figure 8e) emerge in many regions of the parameter space (Figure 9c). At high noise and small field of view ($\eta\Delta t/\omega = 4.5$, $\phi = 10°$), a disordered state where particles have random orientations is observed. Increasing the noise further ($\eta\Delta t/\omega \geq 9$), the disordered state will invade the entire parameter space (Figure 9d).

4. Discussion

We have shown that models based on only alignment can show milling. In the modified Vicsek model, milling spontaneously emerges from a random starting configuration if the field of view of individuals is reduced to intermediate values ($\phi \sim 200°$), and if the maximal angular velocity is reduced such that the ratio of speed to maximal angular velocity $v/(r\omega) \sim 1$.

The necessity of limiting the field of view of particles to obtain milling is in line with findings by Barberis and Peruani [11] for a model based on attraction only. Further, a

decrease of the field of view has been shown to result in milling that is more robust (i.e. for a wider range of parameters) in a model with avoidance, alignment, and attraction [18] and in a model with attraction only it has been shown to result in milling with more complex shapes [9].

Yet, in contrast to our findings, there are also other models, where milling emerges for individuals with a complete field of view ($\phi = 360°$) [9, 18, 19, 24, 25]. All these models are not based on alignment only, but include more interaction types, such as alignment or avoidance, or both.

After sufficient simulation time, our system always reaches either a stable milling state or a stable non-milling state. We do not observe oscillations between milling and non-milling states, as have been shown by Gautrais and coworkers [19]. These oscillations may be attributed to the presence of attraction-interaction and complete field of view ($\phi = 360°$) in that model. The precise mechanisms that lead to this critical instability remain unclear, however.

The observed behavior of individuals in models of collective motion (self-propelled particle models) resembles much the motion of real animals: models can be built to mimic the motion of rod-like bacteria such as *E. coli* (using for example elongated particles and excluded-volume interactions) [30, 31, 32] or rather to mimic the motion of fish in schools (using for example avoidance, alignment and attraction interactions) [6]. Our findings indicate that if fish were only aligning with school members, their limited field of view [33], and limited maximal angular velocity [34] already would induce them to form circular mills. In nature, however, we see more complex shapes of mills than circular mills: mills can have elliptic and irregular shapes, and can vary in both their diameter and their thickness [15, 16]. Our model does not reproduce these non-circular mills. Non-circular mills are for instance generated in models where individuals interact only via attraction [9, 10, 11], and in models that include avoidance, alignment, and attraction [17, 18, 19]. The variation in shape (non-circular mills) observed in nature may therefore be due to the contribution of further interactions beyond alignment, like avoidance and attraction.

In nature, fish form mills which extend in all the three spatial dimensions. In computational models, milling has been shown in models in two dimensions [9, 11, 19, 24, 25], as well as in three dimensions [18]. An open question is if (and how) our results extend to three dimensions, namely if in three dimensions milling can be obtained making use of alignment only.

5. Conclusions

Milling, a rotating circular formation of individuals, is a pattern of collective motion that has often been observed in nature. Several theoretical models, which mostly include attraction, alignment, and avoidance, have produced milling behaviour, but the emergence of milling has never been studied in models of self-propelled particles with alignment only.

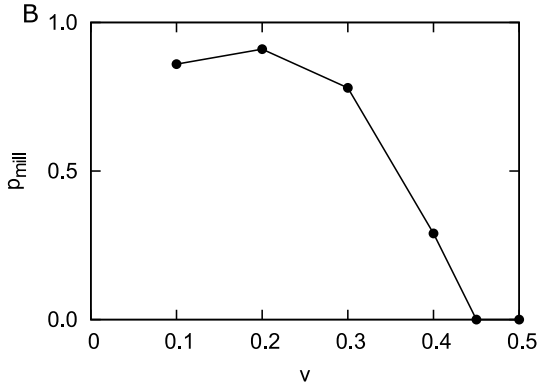

Figure A1. Milling proportion p_{mill} as a function of speed v at constant ratio of speed to maximal angular velocity $v/(r\omega) = 0.9$ (computed over 100 runs, at $\phi = 180°$, $\eta\Delta t/\omega = 0$, $\rho = 2.5$).

Here we have shown for the first time that making minimal modifications to the Vicsek model, a model of self-propelled particles based on alignment only, milling can be obtained. We have demonstrated that by reducing the field of view and reducing the maximal angular velocity, milling spontaneously emerges.

Our results are of theoretical interest and practical relevance, since they give insight in the mechanisms underlying the spontaneous emergence of circular motion in living systems of self-propelled particles.

Acknowledgements

We would like to thank H. Hildebrandt, T. Versluijs, R. Mills, R. Storms, and V. Lecheval for nice and useful discussions.

Appendix

Appendix A.1. Speed range choice

In order to obtain milling, the speed has to be larger than zero but small enough ($v\Delta t/r \ll 1$), since at $v = 0$ particles do not move and thus do not mill, while for $v \to \infty$ we get complete mixing, and thus no milling. We measure the milling proportion as a function of particle speed, at constant speed to maximal angular velocity ratio $v/(r\omega) = 0.9$, for particles moving without noise. We note that for $v > 0.3$ the milling proportion starts to decrease and is zero for $v > 0.45$ (Figure A1). Therefore we have chosen to perform our investigation using $\omega = 10°/\Delta t$ and $0.05 \leq v \leq 0.35$ (velocities are expressed in units of $r/\Delta t$).

Appendix A.2. Milling state

As discussed in Section 2.3, in order to detect particles rotating in mills, a threshold on m_a alone does not suffice. When particles rotate in mills, the average momentum m_a is

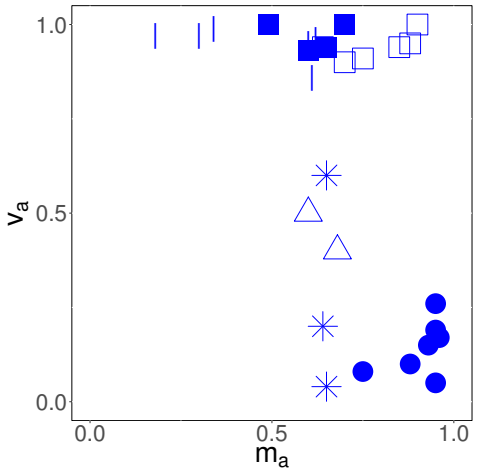

Figure A2. Average velocity v_a and average momentum m_a for different collective patterns. The angular velocity and the particle density are constant, $\omega = 10°/\Delta t$ and $\rho = 2.5$ (system size $L = 20$). Vertical lines: lines ($\phi = 10°$, lines which have smaller m_a are obtained without noise ($\eta\Delta t/\omega = 0$), while lines which have $m_a \simeq 0.6$ are obtained with noise $\eta\Delta t/\omega = 0.5$), circles: stable milling ($v/(r\omega) = 1.5$ and $v/(r\omega) = 0.5$, $\phi = 180°$, $\eta\Delta t/\omega = 0.5$), full squares: flocks ($v/(r\omega) = 1.5$, $\phi = 360°$, $\eta\Delta t/\omega = 0.5$), triangles: fronts ($v/(r\omega) = 0.5$, $\phi = 10°$, $\eta\Delta t/\omega = 0.5$), empty squares: bands ($v/(r\omega) = 1.5$, $\phi = 180°$ and $\phi = 90°$, $\eta\Delta t/\omega = 4.5$), stars: disordered state (disordered states with $v_a > 0.1$ are obtained with $v/(r\omega) = 1.5$, $\phi = 360°$, $\eta\Delta t/\omega = 9$, while disordered states with $v_a < 0.1$ are obtained with $v/(r\omega) = 1.5$, $\phi = 360°$, $\eta\Delta t/\omega = 18$).

larger than 0.75 *and* the average velocity v_a is smaller than 0.5 (see Figure A2). The disordered state with high rotational noise ($\eta\Delta t/\omega = 18$) corresponds to $m_a \simeq 0.6$ and $v_a \simeq 0$, the disordered state with lower rotational noise ($\eta\Delta t/\omega = 9$) corresponds to $m_a \simeq 0.6$ and $v_a \simeq 0.6$, bands happen at $m_a \geq 0.7$ and $v_a \geq 0.9$, flocks at $0.5 \leq m_a \leq 0.7$ and $v_a \geq 0.9$, lines without noise ($\eta\Delta t/\omega = 0$) at $m_a \leq 0.4$ and $v_a \geq 0.9$, lines with noise ($\eta\Delta t/\omega = 0.5$) at $m_a \simeq 0.6$ and $v_a \geq 0.8$, and fronts at $m_a \simeq 0.6$ and $v_a \simeq 0.5$ (see Figure A2). There is no general (i.e. with all collective patterns) one-to-one correspondence between the measured values of m_a and v_a and collective patterns, as the overlap between fronts and disordered state, as well as the overlap between lines and flocks show. Though the correspondence is one-to-one if we consider the values of m_a and v_a and milling/non-milling state (milling $\iff$ $v_a < 0.5$ and $m_a > 0.75$).

Appendix A.3. Number of time-steps and stationary state

The results presented in section 3 have been obtained running simulations of 2000 steps and taking time averages of the average velocity and average momentum in the last 500 steps, having made sure that the stationary state has been already reached (see Figure A3). The relaxation times of the system reaching the milling state and the relaxation times of the system reaching other collective patterns are similar.

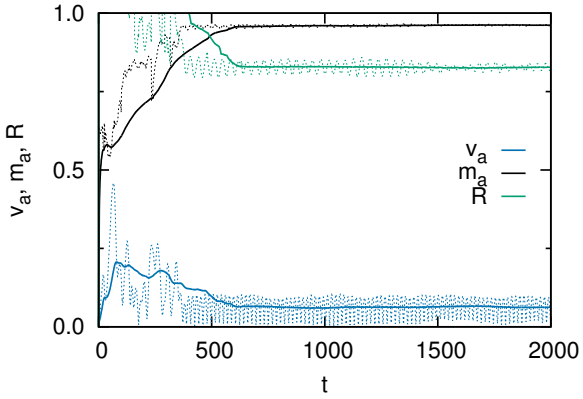

Figure A3. Average velocity v_a (dashed blue line), average momentum m_a (dashed black line), average distance from cluster center R (dashed green line), and their time averages (solid lines) over the previous 500 steps as a function of simulation time t (for $t < 500$ the average is performed from 0 to t). Particles reach a milling state, $\phi = 180°$, $v/(r\omega) = 0.8$, $\eta\Delta t/\omega = 0.5$, $\rho = 2.5$.

References

[1] Vicsek T and Zafeiris A 2012 *Phys. Rep.* **517** 71 – 140
[2] Sumpter D J 2010 *Collective animal behavior* (Princeton University Press)
[3] Krause J and Ruxton G D 2002 *Living in groups* (Oxford University Press)
[4] Camazine S 2003 *Self-organization in biological systems* (Princeton University Press)
[5] Huth A and Wissel C 1992 *Journal of theoretical biology* **156** 365–385
[6] Hemelrijk C K and Hildenbrandt H 2008 *Ethology* **114** 245–254
[7] Hildenbrandt H, Carere C and Hemelrijk C K 2010 *Behavioral Ecology* **21** 1349–1359
[8] Calovi D S, Lopez U, Ngo S, Sire C, Chaté H and Theraulaz G 2014 *New Journal of Physics* **16** 015026
[9] Strömbom D 2011 *Journal of theoretical biology* **283** 145–151
[10] Strömbom D, Siljestam M, Park J and Sumpter D J 2015 *The European Physical Journal Special Topics* **224** 3311–3323
[11] Barberis L and Peruani F 2016 *Physical review letters* **117** 248001
[12] Romenskyy M and Lobaskin V 2013 *The European Physical Journal B* **86** 91
[13] Romensky M, Lobaskin V and Ihle T 2014 *Physical Review E* **90** 063315
[14] Pearce D J and Turner M S 2015 *Journal of The Royal Society Interface* **12** 20150520
[15] Delcourt J, Bode N W and Denoël M 2016 *The Quarterly review of biology* **91** 1–24
[16] Tunstrøm K, Katz Y, Ioannou C C, Huepe C, Lutz M J and Couzin I D 2013 *PLoS computational biology* **9** e1002915
[17] Kunz H, Züblin T and Hemelrijk C K 2006 On prey grouping and predator confusion in artificial fish schools *Proceedings of the Tenth International Conference of Artificial Life. MIT Press, Cambridge, Massachusetts*
[18] Couzin I D, Krause J, James R, Ruxton G D and Franks N R 2002 *Journal of theoretical biology* **218** 1–11
[19] Gautrais J, Jost C and Theraulaz G 2008 Key behavioural factors in a self-organised fish school model *Annales Zoologici Fennici* vol 45 (BioOne) pp 415–428
[20] Shimoyama N, Sugawara K, Mizuguchi T, Hayakawa Y and Sano M 1996 *Physical Review Letters* **76** 3870
[21] Levine H, Rappel W J and Cohen I 2000 *Phys. Rev. E* **63**(1) 017101
[22] D'Orsogna M R, Chuang Y L, Bertozzi A L and Chayes L S 2006 *Physical review letters* **96** 104302

[23] Carrillo J, D'Orsogna M and Panferov V 2009 *Kinetic and Related Models* **2** 363–378
[24] Newman J P and Sayama H 2008 *Physical Review E* **78** 011913
[25] Cheng Z, Chen Z, Vicsek T, Chen D and Zhang H T 2016 *New Journal of Physics* **18** 103005
[26] Czirók A, Ben-Jacob E, Cohen I and Vicsek T 1996 *Physical Review E* **54** 1791
[27] Czirók A and Vicsek T 2000 *Physica A: Statistical Mechanics and its Applications* **281** 17–29
[28] Vicsek T, Czirók A, Ben-Jacob E, Cohen I and Shochet O 1995 *Phys. Rev. Lett.* **75** 1226
[29] Grossmann R, Schimansky-Geier L and Romanczuk P 2012 *New Journal of Physics* **14** 073033
[30] Angelani L, Costanzo A and Di Leonardo R 2011 *EPL* **96** 68002
[31] Costanzo A, Di Leonardo R, Ruocco G and Angelani L 2012 *Journal of Physics: Condensed Matter* **24** 065101
[32] Costanzo A, Elgeti J, Auth T, Gompper G and Ripoll M 2014 *EPL* **107** 36003
[33] Domenici P and Blake R W 1993 *Journal of Experimental Biology* **177** 253–272
[34] Domenici P and Blake R W 1991 *Journal of Experimental Biology* **156** 187–205